FAST AND EASY INTEGRATION AND CLASSIFICATION OF HYPERSPECTRAL OPTICAL AND THERMAL DATA: A MINERAL MAPPING CASE STUDY

Veronika Kopačková(a), Lucie Koucká(a), Jan Jelének(a), Jan Hanuš(b)

Remote Sensing Department, Czech Geological Survey, Prague 11821, Czech Republic(a)
Global Change Research Institute CAS - CzechGlobe, Belidla 986/4a, Brno, Czech Republic(b)

ABSTRACT

Independent spectral analysis is usually employed to analyse hyperspectral optical (visible: VIS, near infrared: NIR, shortwave infrared: SWIR) and thermal (longwave infrared: LWIR) data. The integration of the spectral information provided by different wavelength ranges and the subsequent complex classification still remains challenging. In this paper we will demonstrate the benefits of mineral classification employed to optical and thermal hyperspectral data (CASI and SASI: 0.4-2.5 μm; TASI: 8.6-11.5 μm) when using new tools (QUANTools) developed at the Czech Geological Survey (CGS). In this case study, the same approach was employed as published by Kopačková and Koucká (2017) [1], however, previously hyperspectral optical data were used together with multispectral long-wave infrared (LWIR) data. In this paper we demonstrate that the new concept, which was recently introduced, can be directly employed to CASI/SASI/TASI hyperspectral datasets and provide results in terms of mineral classification in a quick and easy way.

Index Terms— imaging spectroscopy, optical spectral region, thermal infrared spectral region, mineral mapping, data integration, CASI, SASI, TASI

1. INTRODUCTION

Optical and thermal hyperspectral data, when used together, allow different varieties of minerals to be mapped and thus allow lithology mapping in a more complex way. Considering mineral mapping, the majority of the previous work done for diverse spectral data has mainly focused on single-wavelength- range data [2]. Few studies have taken advantage of data from the full VIS/NIR, SWIR, and LWIR spectral range, whereas in most cases the different spectral ranges were analysed and interpreted separately [3,4] and the full-range information was not combined into a single integrated data product. Recently, Kruse [5] proposed integrating the individual mapping results derived from AVIRIS (VIS/NIR/SWIR) and HyTES data (LWIR) and combining them using geologically directed logical operators. In the following study by McDowell and Kruse [2], spectral information from the individual VIS, NIR, SWIR and LWIR ranges was first analysed independently and then the resulting compositional information, in the form of image endmembers and apparent abundances, was integrated using ISODATA cluster analysis. Recently, a new concept integrating HyMAP and AHS imaging data was introduced [1] allowing automatic detection of the multiple absorption features though the VIS/NIR/SWIR and LWIR ranges and their consequent integration. This study looks at whether this new concept/approach can be directly employed to hyperspectral optical and thermal data (CASI/SASI/TASI).

2. HYPERSPECTRAL OPTICAL AND THERMAL DATA SETS

Airborne hyperspectral data were acquired in June 2017 by the FLIS infrastructure (Czech Globe) over the abandoned Lítov dump, Sokolov lignite basin, Czech Republic. The suite of airborne imaging spectroradiometers (hyperspectral system) consisted of three sensors produced by the Canadian company ITRES Research Limited. The first sensor, CASI-1500, acquires data in the VNIR region. The second sensor, SASI-600, acquired data in the SWIR region and the last sensor TASI-600 covers the thermal infrared (LWIR) spectral region. Radiometric and geometric corrections as well as atmospheric corrections were performed to all hyperspectral data; in addition the thermal (LWIR) data were also transformed to temperature values.

The first step in hyperspectral data pre-processing were radiometric corrections, when digital numbers (DN) acquired by sensors are converted to physical values of radiance [$\mu W\ cm^{-2}\ sr^{-1}\ nm^{-1}$]. The next step were atmospheric corrections which are performed by means of the MODTRAN radiative transfer model [6]. The VNIR and SWIR surface reflectance as well as kinetic temperature and emissivity were finally georeferenced to the UTM coordinate system. The resulting ground pixel resolution of the image CASI, SASI and TASI datasets was 2 m. a more detailed description of the CzechGlobe pre-processing chain could be found in [7].

3. METHODS

To map multiple absorption features over the different regions of the electromagnetic spectrum (EMS), namely absorption wavelengths and depths, the QUANTools toolbox developed at the Czech Geological Survey [1], was utilized. The spectral ranges from which the absorption feature parameters were derived were defined as follows: VIS/NIR (CASI): 0.450–1.300 µm, SWIR (SASI): 2.100–2.400 µm and LWIR (TASI): 8.500–11.500 µm. Similarly, as described in Kopačková and Koucká [1], noise detection and correction was employed to the VIS/NIR reflectance (0.450–1.300 µm). The number of absorption features to be mapped in the VNIR and SWIR regions was set to 3, over the thermal region (8.500–11.500 µm) 4 absorption features were mapped. Two new raster datasets were derived for each spectral range, one having the two major absorption wavelengths assigned to it and the second a raster dataset with the corresponding absorption depths.

After absorption feature mapping, the same processing and classification was employed as described in [1]. The MNF transformation was used to comprise all absorption wavelength/depth matrices derived on the basis of the CASI/SASI/TASI data sets. The first three MNF bands were further visually analysed to identify training areas (ROIs) representing different material/surfaces. These were defined as representative pixels of different colour clusters/regions. The ROIs were then used for further supervised classification (non-parametric supervised parallelepiped classification).

In the last step, the classification was overlaid over the original CASI, SASI and TASI image data and the average spectrum from the CASI, SASI and TASI image data was computed for each class to (i) ensure that each class represents a different surface material and (ii) to be able to describe the mineral composition of each class when interpreting the spectral property.

4. RESULTS

As described in the Methods an MNF transformation was employed to the absorption feature mapping results over the VIS/NIR/SWIR (CASI/SASI) and LWIR (TASI) spectral ranges. The ROIs were created using the RGB colour compositions of the first 3 MNF bands and consequently used for supervised parallelepiped classification. As a result, 12 classes were mapped (Figure 1). The spectral property of these classes (average class spectrum) is displayed in Figures 2-4.

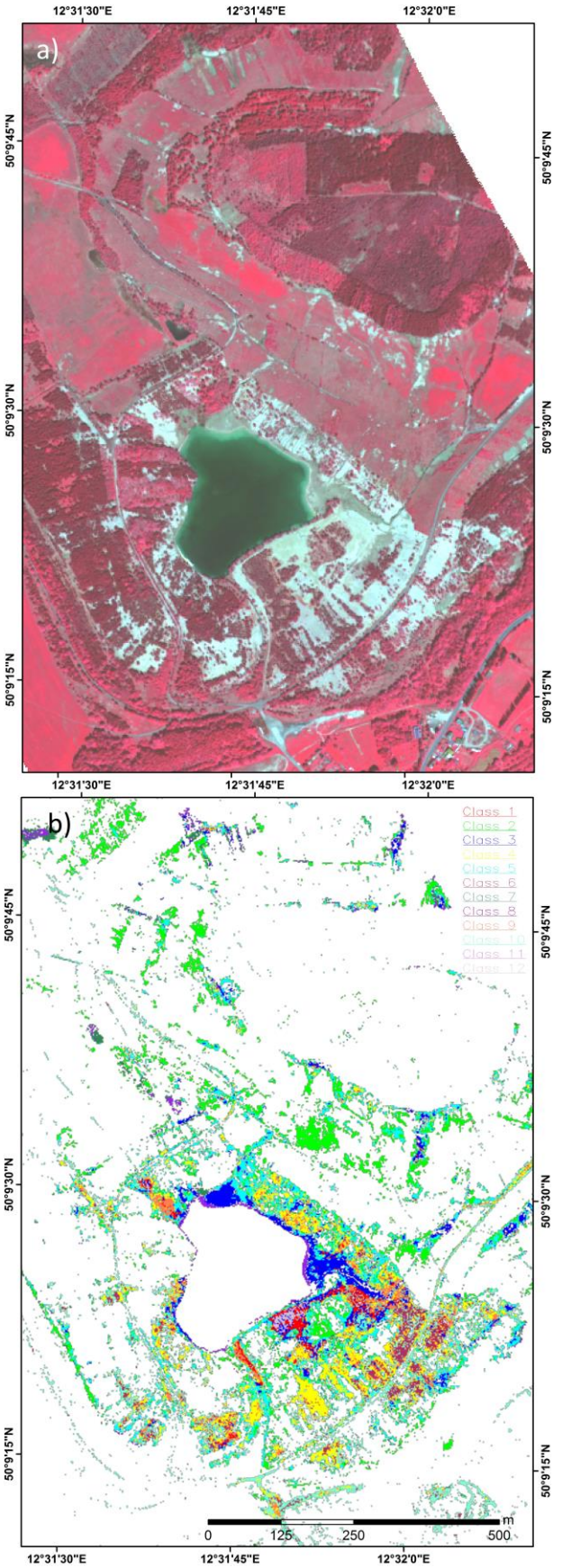

Figure 1: Lítov dump mineral mapping using CASI/SASI/TASI data, 12 mineral classes were identified based on the variability among the absorption features present over the VNIR, SWIR and LWIR spectral regions. The class colours correspond with the colours of the average spectrum computed for each class for CASI (Figure 2), SASI (Figure 3) and TASI (Figure 4). Dense vegetation and water were masked out prior to mineral mapping.

In the VIS/NIR (Figure 2), it can be seen that the average class spectrum exhibits the typical absorption features of secondary Fe^{3+}-bearing minerals. The wavelength position of the first one is placed around 0.500 µm, the second one varies between 0.900 and 1.080 nm indicating a presence of diverse Fe^{3+}-bearing minerals [8, 9]. The absorptions characteristic of organic C are placed around 0.700 µm [10]. In the SWIR (Figure 3), the overtones and combinations of the fundamental OH and H–O–H vibrations can be mainly observed. Based on previous studies [1, 11], these absorption features present in the SWIR, were linked with diverse phyllosilicates (e.g., kaolinite, muscovite and mixtures between these two).

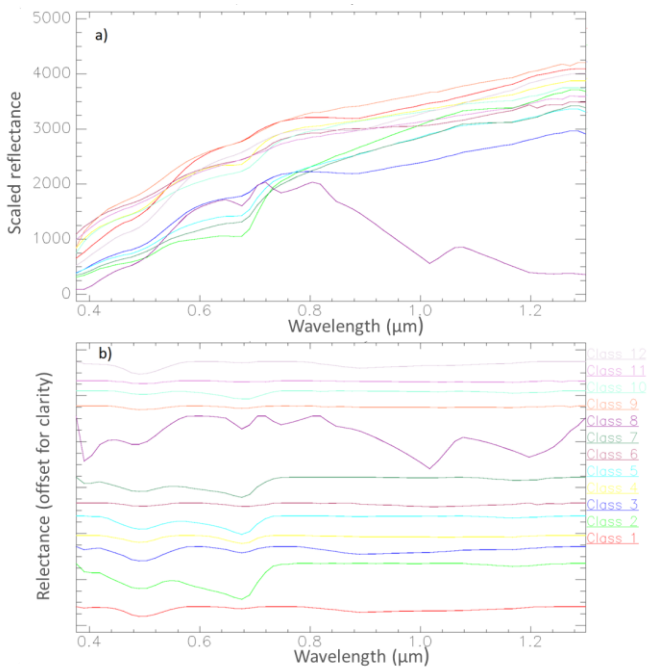

Figure 2: The average class spectrum derived from the CASI data: a) reflectance, b) continuum removal applied to reflectance. The colours correspond with the class colours in Figure 1.

Based on the results published by [1], then, to some extent, the class emissivity can be also linked with minerals. In the LWIR region (Figure 4), quartz affects the emissivity of the bands around 8.6 and 10 µm (high emissivity) as well as at 9.400 µm (low emissivity). The distinct absorption features detectable by the TASI bands placed at 9.800 µm and 10.900 µm characterise kaolinite. Muscovite exhibits absorptions around 9.000 and 9.800 µm.

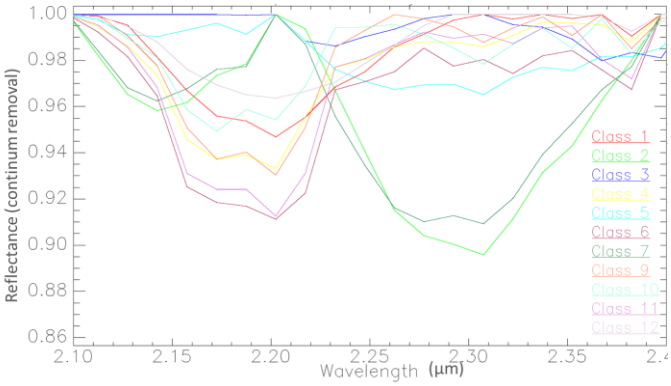

Figure 3: The average class spectrum derived from the SASI data (continuum removal applied to reflectance). The colours correspond with the class colours in Figure 1.

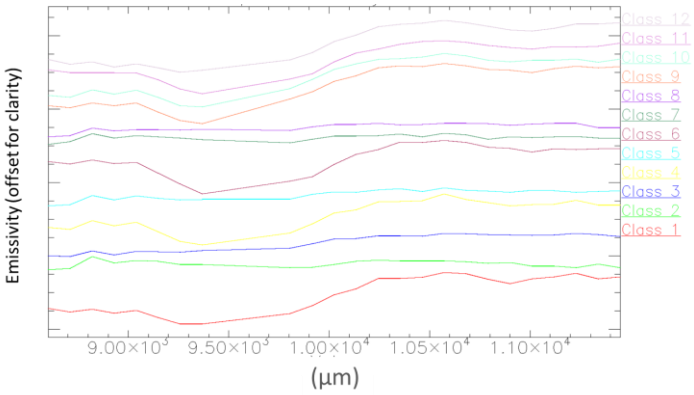

Figure 4: The average class emissivity derived from TASI data (continuum removal applied to emissivity). The colours correspond with the class colours in Figure 1.

5. CONCLUSIONS

In this case study, the same concept as previously published by Kopačková and Koucká [1] was applied to hyperspectral optical and thermal imaging data (CASI, SASI, TASI). The concept is based on the automatic detection of multiple absorption features; moreover it allows quick data processing and classification without requiring endmember definition prior to spectral mapping. As a result 12 mineral classes were identified integrating together the spectral information from CASI, SASI and TASI imaging data. During the spring of 2018, a representative sample for each mapped class will be collected and, consequently, semi-quantitative XRD diffraction analysis will be conducted to resolve the mineralogy in further detail.

It can be concluded that:

- The concept employed previously [1, 12] and in this study does not require prior definition of the endmembers; moreover, there is no need for prior knowledge or data on the specific conditions.
- The concept allows for quick integration and classification of the VIS/NIR, SWIR and LWIR hyperspectral data.
- The approach can increase time/cost efficiency as the validation samples will be collected after image classification targeting, specifically the identified surface variability (e.g., mapped classes).

ACKNOWLEDGEMENTS

The CASI/SASI/TASI data were acquired under a grant from the Ministry of Education Youth and Sports (8G15004). The analysis was conducted under the support of Czech Science Foundation grant 17-05743S. The QUANTools toolbox is available for free (February 2016); if interested, read more at: http://www.cgs-rs.g6.cz/hyperalgo.html or contact quantoolscgs@gmail.com.

11. REFERENCES

[1] Kopačková, V.; Koucká, L. Integration of Absorption Feature Information from Visible to Longwave Infrared Spectral Ranges for Mineral Mapping. Remote Sens., 9, 1006, 2017.

[2] McDowell, M.L.; Kruse, F.A. Enhanced Compositional Mapping through Integrated Full-Range Spectral Analysis. Remote Sens., 8, 757, 2016.

[3] Notesco, G.; Kopačková, V.; Rojík, P.; Schwartz, G.; Livne, I.; Dor, E.B. Mineral classification of land surface using multispectral LWIR and hyperspectral SWIR remote-sensing data. A case study over the Sokolov lignite open-pit mines, the Czech Republic. Remote Sens., 6, 7005–7025, 2014.

[4] Feng, J.; Rogge, D.; Rivard, B. Comparison of lithological mapping results from airborne hyperspectral VNIR-SWIR, LWIR and combined data. Int. J. Appl. Earth Obs. Geoinf., 64, 340–353, 2018.

[5] Kruse, F.A. Integrated visible and near-infrared, shortwave infrared, and longwave infrared full-range hyperspectral data analysis for geologic mapping. J. Appl. Remote Sens., 9, 096005, 2015.

[6] Acharya, P.K., Anderson, G.P., Berk, A. and Shettle, E.P.. MODTRAN® 5.2. 0.0 USER'S MANUAL, 2008.

[7] Hanus, J.; Fabianek, T.; Fajmon, L.; et al. (2016). POTENTIAL OF AIRBORNE IMAGING SPECTROSCOPY AT CZECHGLOBE; Source: XXIII ISPRS Congress, Commission I Volume: 41 Issue: B1 Pages: 15-17 Published: 2016.

[8] Clark, R.N.; King, T.V.; Klejwa, M.; Swayze, G.A.; Vergo, N. High spectral resolution reflectance spectroscopy of minerals. J. Geophys. Res. Solid Earth, 95, 12653–12680, 1990.

[9] Murphy, R.J.; Monteiro, S.T. Mapping the distribution of ferric iron minerals on a vertical mine face using derivative analysis of hyperspectral imagery (430–970nm). ISPRS J. Photogramm. Remote Sens., 75, 29–39, 2013

[10] Kopačková, V.; Ben-Dor, E.; Carmon, N.; Notesco, G. Modelling Diverse Soil Attributes with Visible to Longwave Infrared Spectroscopy Using PLSR Employed by an Automatic Modelling Engine. Remote Sens., 9, 134, 2017.

[11] Kopačková, V. Using multiple spectral feature analysis for quantitative pH mapping in a mining environment. Int. J. Appl. Earth Obs. Geoinf., 28, 28–42, 2014.

[12] Van der Meer, F.D.; Kopačkova, V.; Koucká, L.; van der Werff, H.M.; van Ruitenbeek, F.J.; Bakker, W.H. Wavelength feature mapping as a proxy to mineral chemistry for investigating geologic systems: An example from the Rodalquilar epithermal system. Int. J. Appl. Earth Obs. Geoinf., 64, 237-248, 2018.

.